Single Crystal EPR Study of the Dinuclear Cu(II) Complex [Cu(tda)(phen)](2)center dot H(2)tda (tda = Thiodiacetate, phen = Phenanthroline): Influence of Weak Interdimeric Magnetic...

ARTICLE *in* THE JOURNAL OF PHYSICAL CHEMISTRY A · DECEMBER 2010

Impact Factor: 2.69 · DOI: 10.1021/jp108736p · Source: PubMed

Single Crystal EPR Study of the Dinuclear Cu(II) Complex $[Cu(tda)(phen)]_2 \cdot H_2tda$ (tda = Thiodiacetate, phen = Phenanthroline): Influence of Weak Interdimeric Magnetic Interactions

Nicolás I. Neuman,[†] Mireille Perec,[‡] Pablo J. González,[§] Mario C. G. Passeggi,[†,||] Alberto C. Rizzi,[†] and Carlos D. Brondino*[,†]

Departamento de Física, Facultad de Bioquímica y Ciencias Biológicas, Universidad Nacional del Litoral, Ciudad Universitaria, Paraje El Pozo, S3000ZAA Santa Fe, Argentina, Departamento de Química Inorgánica Analítica y Química Física, Facultad de Ciencias Exactas y Naturales, INQUIMAE, Universidad de Buenos Aires, Ciudad Universitaria, Pabellón II, 1428, Buenos Aires, Argentina, Departamento da Quimica, Requimte/CQFB, Faculdade de Ciências e Tecnologia, Universidade Nova de Lisboa, 2829-516 Caparica, Portugal, and Intec, Conicet-UNL, Güemes 3450, 3000 Santa Fe, Argentina

Received: September 13, 2010; Revised Manuscript Received: November 9, 2010

We report powder and single crystal EPR measurements of $[Cu(tda)(phen)]_2 \cdot H_2tda$ (tda = thiodiacetate, phen = phenanthroline) at 9.7 GHz. This compound consists of centrosymmetric copper(II) ion dimers, weakly ferromagnetically exchange-coupled ($J = +3.2$ cm^{-1}), in which the dimeric units are linked by hydrophobic chemical paths involving the phen molecules. EPR revealed that the triplet spectra are collapsed by interdimeric exchange interactions mediated by that chemical path. Analysis and simulation of the single crystal EPR spectra were performed using Anderson's exchange narrowing model, together with statistical arguments. This approach allowed us to interpret the spectra modulated by the interdimeric interactions in situations of weak, intermediate, and strong exchange. We evaluated an interdimeric exchange constant $J' = 0.0070(3)$ cm^{-1}, indicating that hydrophobic paths can transmit weak exchange interactions between centers at relatively long distances of the order of ~10 Å.

Introduction

The study of exchange-coupled copper(II) dinuclear systems is an important subject of research in both inorganic and bioinorganic chemistry, due to their relevance in molecular magnetism and in the study of copper proteins.[1−4] The physicochemical theories that explain the magnetic coupling phenomenon in these type of systems have been established in the middle of the past century[5−8] and have been widely used in the characterization of dinuclear copper compounds.[9−12]

For a dinuclear copper(II) system ($S = 1/2$ ion pair), the spin−spin coupling is determined by the isotropic exchange constant J and by anisotropic interactions such as dipolar and anisotropic and antisymmetric exchange. The isotropic exchange interaction ($\mathbf{H}_{ex} = -J\mathbf{S}_1 \cdot \mathbf{S}_2$) splits the singlet state from the triplet state of the dimer by an energy amount J, whereas the remaining interactions cause the threefold degeneration of the triplet state to be removed even in zero magnetic field (ZFS). Additional splitting of the energy levels can be produced by the hyperfine interaction with the copper nucleus ($I = 3/2$). Furthermore, in weakly exchange-coupled dimers the anisotropic interactions mix appreciably the singlet and triplet states, which therefore cannot be considered pure in character. However, singlet−triplet nomenclature will be used throughout the text for simplicity.

The magnetic characterization of dimeric systems is usually performed on solid state samples by magnetic susceptibility measurements and also, though less frequently, by EPR spectroscopy. While the former is used principally for evaluating the intradimeric isotropic exchange interaction J, the latter is more appropriate to evaluate the above-mentioned anisotropic interactions. Particularly, when EPR spectroscopy is performed on oriented single crystal samples, it can be used to calculate the eigenvalues and eigenvectors of the tensorial magnitudes associated with such interactions.[6,7,13−17] In undiluted magnetic systems, the dimeric units of the crystal lattice may interact with their neighbors through different kinds of chemical paths that may transmit weak exchange interactions, hereafter designated J'. These interactions should be considered in the analysis of the data, since they can introduce modifications in the magnetic behavior of the dimer.[14,16,17] For thermodynamic magnetic measurements, the problem is well-known and can be easily accounted for by including in the Hamiltonian an energetic term describing the intermolecular interactions J' in the molecular-field approximation.[7] In contrast, the analysis by EPR can be more complicated because interdimeric exchange interactions may produce merging effects of the EPR triplet spectra, a phenomenon that has been previously well documented.[14,16−23] For weak exchange ($J' <$ ZFS), the two EPR resonance lines of the triplet state are shifted to the center of the spectra and broadened; the larger J', the larger the shift and broadening. In contrast, for strong exchange ($J' >$ ZFS) the two lines merge into one. Similar spectral changes have also been observed in EPR measurements of interacting dimers as a function of temperature, since the effective J'-value depends on the thermal equilibrium density ρ of triplet states, a phenomenon which has been documented in moderately strong antiferromagnetically coupled dimers.[16,17,20] The EPR spectra of these systems at temperatures with low ρ values ($kT < J$) show well-resolved triplet spectra, which are averaged out at higher temperatures

* To whom correspondence should be addressed. E-mail: brondino@fbcb.unl.edu.ar. Fax: +54-342-4575221. Tel.: +54-342-4575213.
[†] Universidad Nacional del Litoral.
[‡] Universidad de Buenos Aires.
[§] Universidade Nova de Lisboa.
[||] Conicet-UNL.

10.1021/jp108736p

($kT > J$) by the interdimeric triplet−triplet exchange interaction (J') to give a single resonance line at the center of the low temperature spectra.

We report here a single crystal EPR study of the dimeric copper(II) compound $[Cu(tda)(phen)]_2 \cdot H_2tda$ (tda = thiodiacetate, phen = phenanthroline). The compound consists of ferromagnetically exchange-coupled centrosymmetric copper(II) dimers with intradimer isotropic exchange constant $J = +3.2$ cm^{-1}.[24] The analysis of the angular variation of the triplet resonance line positions revealed the presence of weak interdimeric exchange interactions and that the ZFS is only determined by the intradimer dipole−dipole interaction. We present a theoretical model based on Anderson's theory of exchange narrowing combined with statistical arguments to interpret how EPR spectra of a dimeric system are influenced by weak interdimeric exchange interactions in situations of weak, intermediate, and strong exchange.

Experimental Methods

Single crystals of $[Cu(tda)(phen)]_2.H_2tda$ were obtained as reported elsewhere.[24] The morphology of the single crystals, necessary to orient the sample for the EPR experiment, was determined by measuring the angles between crystal faces using a Carl Zeiss Axiolab goniometric microscope. The monoclinic crystals are elongated prisms that grow along the c axis and have lateral faces (110) and ($\bar{1}$10), with the angle between the ca^* plane ($a^* = b \times c$) and the (110) plane being 36.9°.

Powder and oriented single crystal samples were measured at 9.7 GHz on a Bruker ER 200 spectrometer equipped with an Oxford helium continuous-flow cryostat. Positions and widths of the resonance lines were obtained by least-squares fitting the field derivative of one or two Lorentzian functions to the spectra. EPR spectra were analyzed with the EasySpin toolbox based on MATLAB.[25] Molecular graphics were made with Mercury.[26] Single crystal EPR spectra were taken in the a^*b, ca^*, and cb crystal planes by gluing the (110) face of a single crystal (approximately 0.7 × 0.7 × 1.5 mm) to a specially designed rexolite sample holder, with an angle of 36.9° (see above). The sample holder was glued to a pedestal and positioned at the center of the microwave cavity, and the magnet was rotated in the three crystal planes. Powder samples for EPR were obtained by grinding single crystals.

Results and Discussion

Crystal and Molecular Structure. A brief description of the crystal structure is presented in order to interpret the EPR experiment. The compound $[Cu(tda)(phen)]_2 \cdot H_2tda$, hereafter Cu(tda)(phen), crystallizes in the monoclinic space group $C2/c$, $z = 4$.[24] The crystal structure consists of centrosymmetric copper(II) ion dimers in which copper ions are 3.342 Å apart, linked by two μ-O bridges (Figure 1). Each copper atom is in a distorted octahedral environment of the N_2O_3S type, where the equatorial positions are occupied by N atoms (N1 and N2) and O atoms (O2 and O4) from the 1,10-phenanthroline and thiodiacetate ligands, respectively. The axial positions are occupied by the S1 and O2 atoms from the two thiodiacetate molecules related by the inversion center. The Cu(II) ions share the O2 ligands, which are in apical position for one Cu atom and in equatorial position for the other.

There are four chemically identical dimers in the unit cell related by the symmetry operations of the space group $C2/c$ (Figure 2). The dimers related by a translation (type A(B)) are magnetically equivalent. Dimers A and B are related by a 180° rotation around the b axis plus a translation (0, 0, 1/2) and hence are magnetically nonequivalent.

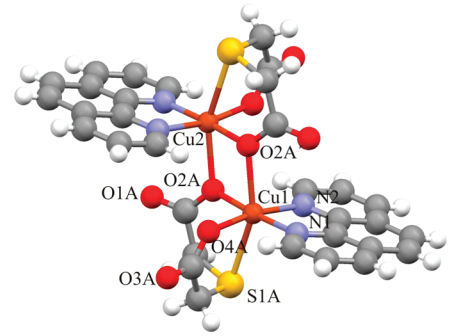

Figure 1. Cu(tda)(phen) dimer molecule showing relevant atom labels. The atoms related by an invertion are labeled with a colon.

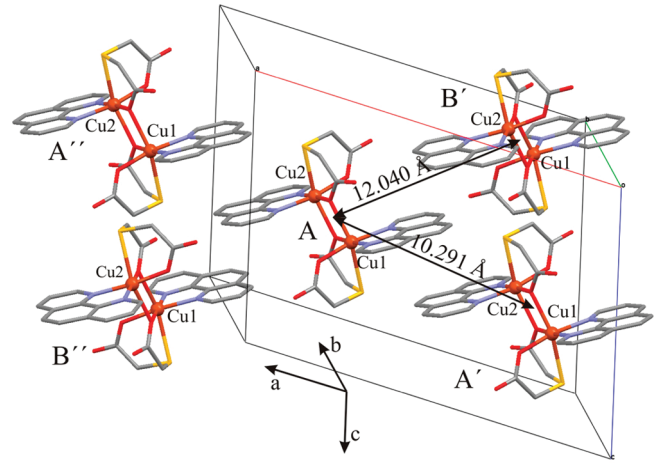

Figure 2. Perspective of the crystal unit cell showing a Cu(tda)(phen) dimer with its four nearest neighbors.

The phenanthroline planes between molecules of the same dimer type (A−A or B−B) are parallel and 3.431 Å apart, whereas the phenanthroline planes of different dimer types (A−B) deviate by 4.32°, with the shortest distance between them being 3.482 Å. These distances strongly suggest delocalized $\pi-\pi$ interactions between aromatic planes. Thus, dimer A(B) may interact with two type A(B) dimers and two type B(A) dimers (Figure 2), with distances between dimers (measured from their inversion centers) of 10.291 and 12.040 Å for A−A(B−B) and A−B dimers, respectively. Nonadjacent A and B dimers are also bridged by a long mixed chemical path involving two hydrogen bonds (O−H···O distance = 2.58(6) Å, O−H···O angle = 177(6)°) and a thiodiacetic acid molecule (not shown). This chemical path of 15 diamagnetic atoms, connecting copper ions at 19.321 Å, is too long to transmit exchange interactions and therefore will not be considered in the analysis of the EPR data.

Powder and Single Crystal EPR Spectra. ***Spin Hamiltonian.*** Figure 3 shows the EPR spectrum of a powder sample of Cu(tda)(phen) at room temperature. Although the typical half-field resonance at $g \sim 4$ is observed (see inset in Figure 3), as expected for the forbidden transition $\Delta m_s = \pm 2$ of a dimer, the more intense signal at $g \sim 2.20$ is not typical for a triplet state[27] resembling the characteristic signals of exchange-coupled extended compounds.[28,29] Similar spectra were observed in the temperature range 4−200 K, indicating that even at very low temperatures variations in spin triplet density are not significant enough to alter the effective spin exchange interactions that determine the EPR line shapes.

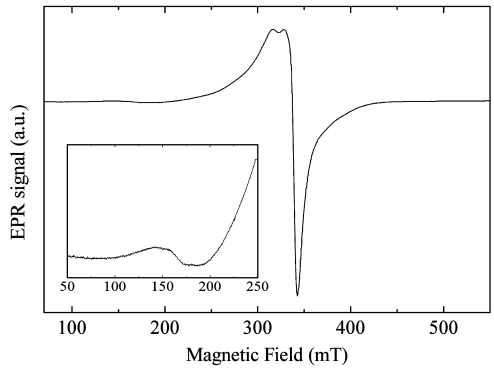

Figure 3. Powder EPR spectrum of Cu(tda)(phen) at room temperature. The inset shows the signal at half-field.

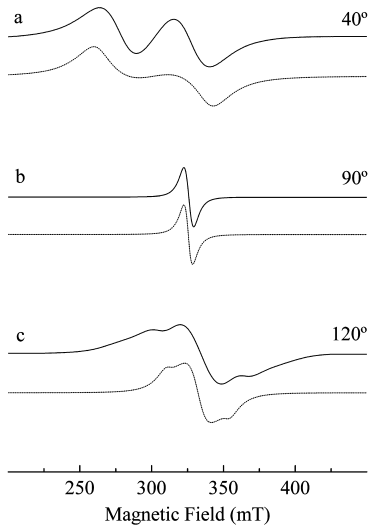

Figure 4. Representative EPR spectra (solid lines) obtained in the *ca** crystal plane at three different magnetic field orientations together with simulation (dotted lines).

Figure 4 shows representative single crystal EPR spectra of Cu(tda)(phen) in the *ca** plane (the complete angular variation of the spectra is given in the Supporting Information, Figure S1). Spectra were least-squares fitted assuming either one or the sum of two Lorentzian-shaped lines having the same intensity, with the exception of those like spectrum c, which were obtained at certain magnetic field orientations, as will be discussed later. The positions of the resonance lines obtained in the *ca** and *cb* planes as a function of the magnetic field orientation are shown in Figure 5. For the spectra with a pattern such as spectrum c, only the position of the central line is shown. The spectra in the *a*b* plane (not shown) show a single Lorentzian line for most magnetic field orientations.

The EPR spectra of Cu(tda)(phen) result from two magnetically nonequivalent copper(II) dimers. In the absence of interdimeric exchange interactions, four-line EPR spectra associated with the nonequivalent dimers should be observed for an arbitrary magnetic field orientation in the single crystal experiment, except for those orientations lying on the *ca** plane and along the symmetry *b* axis, where the dimers are magnetically equivalent and consequently two lines are expected. However, many spectra in the *ca** plane consist of a single Lorentzian line (Figure 5a), indicating that the EPR triplet spectra are collapsed by interdimeric exchange. A similar conclusion can be obtained from the analysis of the *cb* (Figure 5b) and *a*b* (not shown) planes, where one- or two-line spectra

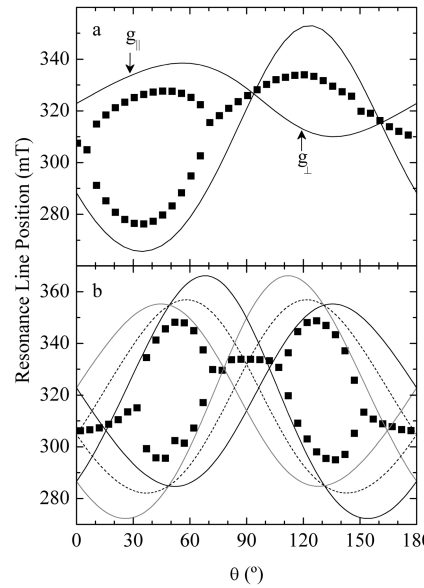

Figure 5. EPR resonance line positions (solid squares) as a function of the magnetic field orientation in the *ca** (a) and *cb* (b) planes. The solid lines correspond to resonance line positions assuming isolated dimers. In the *cb* plane, black and gray solid lines correspond to dimers A and B, respectively. Dashed lines correspond to the average between the closest lines of nonequivalent dimers.

are observed instead of the expected four-line ones, confirming the interdimeric exchange interaction between nonequivalent dimers A and B.

The effective spin Hamiltonian for a system containing four symmetry-related isolated dimers of coupled identical $S = 1/2$ ions per unit cell can be written as

$$\mathbf{H}_{\text{dim}}^{\text{isolated}} = \sum_{\alpha} [\mu_B(\vec{\mathbf{S}}_{\alpha 1} + \vec{\mathbf{S}}_{\alpha 2})\cdot\mathbf{g}_\alpha\cdot\vec{\mathbf{B}} + \vec{\mathbf{S}}_{\alpha 1}\cdot(J\mathbf{I} + \mathbf{D}_\alpha)\cdot\vec{\mathbf{S}}_{\alpha 2}] \quad (1)$$

where the sum over the number N of unit cells in the crystal is omitted for simplicity. In eq 1, α = A, A′, B, B′ corresponds to each type of dimer in the unit cell, $\mathbf{g}_\alpha$ is the **g**-tensor associated with the A or B units ($\mathbf{g}_{\alpha 1}$ and $\mathbf{g}_{\alpha 2}$ tensors are identical because of the inversion center and hence identical to $\mathbf{g}_\alpha$), J is the isotropic exchange interaction constant between Cu1 and Cu2, **I** is the unit matrix, and $\mathbf{D}_\alpha$ is a second rank symmetric tensor with a trace of zero, which can contain contributions from both dipole−dipole interaction and anisotropic exchange.[7] Eq 1 is written in an uncoupled representation; the ZFS term can alternatively be written in a coupled representation ignoring the singlet state as $\vec{\mathbf{S}}\mathbf{D}\vec{\mathbf{S}}$, where $\vec{\mathbf{S}} = \vec{\mathbf{S}}_{\alpha 1} + \vec{\mathbf{S}}_{\alpha 2}$ and **D** is half the **D**-tensor defined in eq 1. $\vec{\mathbf{S}}\mathbf{D}\vec{\mathbf{S}}$ can alternatively be written as $D(\hat{S}_Z^2 - (1/3)\hat{S}^2) + E(\hat{S}_X^2 - \hat{S}_Y^2)$, where D and E are scalar magnitudes related to the eigenvalues of the D-tensor by $D = (3/2)D_Z$ and $E = (1/2)(D_X - D_Y)$.[27] The hyperfine interactions with the copper nuclei are not included in eq 1 as they were not detected experimentally.

As will be shown later, in this case $\mathbf{D}_\alpha$ is determined only by the dipolar coupling between the Cu(II) ions within each dinuclear unit. Taking only the secular terms of the dipolar interaction, i.e., the terms commuting with the Zeeman energy, and the Zeeman energy sufficiently large compared to the ZFS, eq 1 predicts, in a first-order approximation for isotropic g-factor, two resonance lines separated by

$$\Delta_\alpha = \frac{\frac{3}{2}(\mathbf{z}_\alpha \mathbf{D}_\alpha \mathbf{z}_\alpha)}{g\mu_B} = \frac{3}{2}\frac{g\mu_B}{r^3}(1 - 3\cos^2\theta) \qquad (2)$$

in which $\mathbf{z}_\alpha = \mathbf{B}/||\mathbf{B}||$ is the quantization axis along the magnetic field **B**, r is the intermetal distance, and θ is the angle between r and **B**. In this way, Δ_α is expressed in magnetic field units.[27,30]

As seen in Figure 2, each dimeric unit interacts with four neighboring dimers through hydrophobic interactions, which may present exchange constants in the range 0.04−0.12 cm^{-1}.[31−33] Taking a dimer of type A as a central unit, one of its copper(II) ions (Cu1) interacts with Cu2 ions of the neighboring dimers A′ and B′, while the second copper(II) ion (Cu2) interacts similarly with Cu1 ions belonging to dimers A″ and B″. As the structural data show similar parameters for dimers of the same (A−A or B−B) or different (A−B) types, a single exchange parameter J' will be used in our analysis. Taking into account these interactions, the corresponding interdimeric exchange Hamiltonian centered on dimer A can be written as

$$\mathbf{H}^{exch}_{inter,A} = J'[\vec{\mathbf{S}}_{A1}\cdot(\vec{\mathbf{S}}_{A'2} + \vec{\mathbf{S}}_{B'2}) + \vec{\mathbf{S}}_{A2}\cdot(\vec{\mathbf{S}}_{A''1} + \vec{\mathbf{S}}_{B''1})] \qquad (3)$$

where the subindex *inter* stands for interdimeric interactions. A similar expression can be written for the three remaining dimers in the unit cell. Therefore the full Hamiltonian becomes

$$\mathbf{H} = \mathbf{H}^{isolated}_{dim} + \frac{1}{2}\sum_\alpha \mathbf{H}^{exch}_{inter,\alpha} \qquad (4)$$

where the factor 1/2 accounts for the double counting of the interactions. Interdimer dipolar and anisotropic and antisymmetric exchange interactions should also be included in eq 4. However, as these interactions mainly contribute to the broadening of the resonance lines and not to their position, they are not included in this equation.

The changes introduced in the spectra by the $\mathbf{H}^{exch}_{inter,\alpha}$ term in eq 4 can be interpreted using the "random frequency modulation model" introduced by Anderson.[34−37] For a two-center magnetic system capable of absorption at two frequencies ω_1 and ω_2 with equal transition probabilities, where the two frequencies are jumping back and forth with an exchange frequency ω_{ex} of the order of J'/h, the EPR absorption spectrum in the frequency domain is given by[33]

$$I(\omega) = a\frac{(\omega - \omega_c)^2(\Gamma_1 + \Gamma_2) + 2\delta(\omega - \omega_c)(\Gamma_1 - \Gamma_2) + [\delta^2 + \Gamma_1\Gamma_2 + \omega_{ex}(\Gamma_1 + \Gamma_2)](4\omega_{ex} + \Gamma_1 + \Gamma_2)}{[\delta^2 - (\omega - \omega_c)^2 + \Gamma_1\Gamma_2 + \omega_{ex}(\Gamma_1 + \Gamma_2)]^2 + [(2\omega_{ex} + \Gamma_1 + \Gamma_2)(\omega - \omega_c) + \delta(\Gamma_1 - \Gamma_2)]^2} \qquad (5)$$

where a is an arbitrary intensity factor, $\omega_c = (\omega_1 + \omega_2)/2$, $\delta = (\omega_2 - \omega_1)/2$, and Γ_1 and Γ_2 are the intrinsic line widths of ω_1 and ω_2, respectively. Eq 5 can alternatively be deduced from generalized Bloch equations.[38] Assuming frequency-independent Γ_1 and Γ_2, eq 5 can be converted into the field domain multiplying all the frequency quantities by $h/g\mu_B$, where the g-factor corresponds to that of the gravity center of each spectrum (see the following section). In the particular case of Cu(tda)phen, ω_1, Γ_1 and ω_2, Γ_2 correspond to the positions and line widths, respectively, of each of the two triplet resonance lines when $\omega_{ex} = 0$ and $\delta = \Delta/2 = 3/4(\mathbf{z.D.z})$ (see eq 2). The spectra predicted by eq 5 depend on the ratio δ/ω_{ex}; for $\delta/\omega_{ex} < 1$ (strong exchange), this equation predicts one resonance line at $\omega_c = (\omega_1 + \omega_2)/2$, with a width of M_2/ω_{ex}, where M_2 is the second moment of the interactions contributing to the line width.[35] By contrast, for $\delta/\omega_{ex} > 1$ eq 5 predicts two lines, originally at ω_1 and ω_2, but shifted toward ω_c; the larger ω_{ex}, the larger the shift, and in this case the exchange frequency ω_{ex} yields broadening rather than narrowing. As will be seen later, eq 5 will be used in the analysis of the EPR spectra.

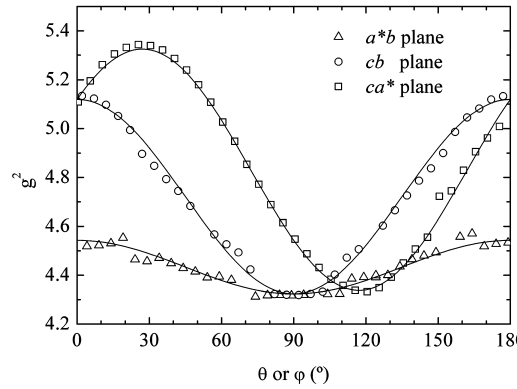

Figure 6. Angular variation of $g^2(\theta, \varphi)$ in the three crystal planes. The data correspond to the crystal **g**-tensor $\mathbf{g} = (\mathbf{g}_A + \mathbf{g}_B)/2$.

TABLE 1: Eigenvalues and Eigenvectors of the Crystal and Molecular g-Tensors in the *a*bc* = *xyz* Crystal Axes System

$g^2_{xx} = 4.543(6)$	
$g^2_{yy} = 4.323(6)$	
$g^2_{zz} = 5.119(6)$	
$g^2_{zx} = 0.401(7)$	
$g^2_{xy} = 0.000(7)$	
$g^2_{zy} = 0.000(7)$	
$g^2_1 = 4.323(6)$	$a_1 = [0.89(6), 0.0(3), -0.46(3)]$
$g^2_2 = 4.338(8)$	$a_2 = [0.0(3), -0.99(7), -0.0(1)]$
$g^2_3 = 5.325(7)$	$a_3 = [0.456(5), 0.000(7), 0.890(2)]$
$g_\parallel = 2.311(1)$	$z_A = [-0.4544, 0.086, 0.887]$
$g_\perp = 2.079(1)$	$z_B = [-0.4544, -0.086, 0.887]$

The Crystal and Molecular g-Tensor. Figure 6 shows the angular variation of the g^2-factors in the three crystal planes, which were obtained from the central position of the spectra and used to obtain the crystal **g**-tensor $\mathbf{g} = (\mathbf{g}_A + \mathbf{g}_B)/2$ by least-squares fitting eq 6 to the data

$$g^2(\theta, \varphi) = g^2_{xx}\sin^2\theta\cos^2\varphi + g^2_{yy}\sin^2\theta\sin^2\varphi + g^2_{zz}\cos^2\theta + 2g^2_{xy}\sin\theta\cos\varphi\sin\varphi + 2g^2_{zx}\sin\theta\cos\varphi\cos\theta + 2g^2_{zy}\sin\theta\sin\varphi\cos\theta \qquad (6)$$

where θ and φ are the polar and azimuthal angles, respectively, in the $a^*bc = xyz$ system. The components of the crystal **g**-tensor are given in Table 1 and were used to obtain the solid lines in Figure 6. The components and orientation of the molecular **g**-tensor were obtained assuming axial symmetry as described elsewhere (see Table 1).[39] The assumption of axial symmetry is based on both the approximately square planar coordination around the copper ions and the similar g-values

obtained along the *b* crystal axis and at $\theta = 120°$ in the *ca** crystal plane, two directions lying approximately on the equatorial ligand plane of the Cu(II) ions. The $g_{||}$ eigenvector deviates by 5.73° from the normal to the equatorial ligand plane confirming our assumption. The molecular **g**-factors found for Cu(tda)(phen) ($g_\perp = 2.079$ and $g_{||} = 2.311$) are similar to those reported for the structurally related Cu(tda)(bipy) ($g_\perp = 2.08$ and $g_{||} = 2.29$)[40] and indicate that the main contribution to the ground state of the copper ions is given by a d_{x2-y2} orbital, where "*x*" and "*y*" axes are defined along the Cu-equatorial ligand bonds.

Interdimer Exchange. The solid lines in Figure 5 correspond to the calculated positions of the resonance lines in the *ca** and *cb* planes as a function of the magnetic field orientation in the absence of interdimer exchange interaction. This calculation was performed using the components of the molecular **g**-tensors (Table 1) and assuming an axial **D**-tensor under the point dipolar approximation considering an isotropic *g*-value ($g_{av} = 2.15$). The same calculation but using the full point dipolar model and anisotropic *g*-values does not show significant differences. As seen in Figure 5, the angular variation of the partially solved resonance lines coincides with the angular variation expected for noninteracting dimers, indicating that the ZFS is determined by the intradimer dipolar interaction. The use of the point dipolar approximation relies on DFT calculations that reproduce satisfactorily the ferromagnetic nature of Cu(tda)(phen) ($J_{calc} = +5.4$ cm^{-1}) and show that the unpaired spin density is mainly localized on the equatorial planes with partial delocalization to the ligands.[41] The eigenvalues and eigenvectors of the $\mathbf{D}_A$ and $\mathbf{D}_B$ tensors used in this calculation are given as Supporting Information (Table S1). The angular variation of the resonance positions in Figure 5 could be well reproduced taking into account that the unique axis of the dipolar tensor deviates 7.2° from the Cu−Cu dimer axis, a fact which can likely originate from covalent effects not considered in the point dipole model.

Figure 5a shows that the largest separation between calculated resonance lines (Δ_t, see eq 2) and the largest experimental separation (Δ_e) occur at the same angle (35°) in the *ca** plane. Furthermore, the largest Δ_e-value is approximately 0.67 times lower than Δ_t, which indicates that, even in the region of maximal line separation, interdimeric exchange interactions are partially collapsing the triplet spectra.

To obtain the interdimer exchange constant J' in Cu(tda)phen, the derivative of eq 5 in magnetic field units was least-squares fitted to the experimental spectra. This was performed with the spectra in the weak exchange regime in the *ca** plane (15°−60° range), as in this region ω_{ex} can be evaluated as an independent fitting parameter. For each spectrum, the positions of the resonance lines in the absence of interdimeric exchange were taken from the solid lines in Figure 5a, whereas the intrinsic line widths Γ_1 and Γ_2 and the exchange frequency ω_{ex} were permitted to float. This procedure reproduced well the experimental spectra (see Figure S2) and yielded an interdimer exchange parameter $\omega_{ex} = (0.021 \pm 0.001)$ cm^{-1}.

The analysis of the data in the *cb* plane (Figure 5b) presents an extra complexity as dimers A and B are not equivalent in this plane, and in the absence of interdimeric exchange interaction, there should be four resonance lines for most magnetic field orientations. However, and similarly to what is seen in the *ca** plane, one- or two-line spectra were observed. The solid lines in Figure 5b correspond to the theoretical angular variation of the resonance lines of dimers A (black lines) and B (gray lines), whereas the dashed lines correspond to the average of the closest lines of different dimers. The two-line spectra show an angular variation similar to that of the average lines, indicating that interdimer exchange is collapsing resonances corresponding to nonequivalent dimers. Also, as observed in the *ca** plane, the experimental separation Δ_e is always lower than the theoretical one, which indicates that the collapsed lines of nonequivalent dimers suffer an additional collapse.

The same procedure applied for the determination of ω_{ex} in the *ca** plane was applied to the data from the *cb* plane, but using as ω_1 and ω_2 the averages of nearest lines (dashed lines in Figure 5b). The result obtained by fitting the derivative of eq 5 to the spectra was $\omega_{ex} = (0.017 \pm 0.001)$ cm^{-1} which, considering the approximate approach, is in good agreement with the value obtained from the analysis of the *ca** plane.

Considering that interdimeric exchange interactions operate only between dimers in triplet states, the interdimeric exchange constant J' can be obtained from the equation $\omega_{ex} = z\rho(J, T)J'$, where $z = 4$ is the number of nearest neighbors of each dimer and $\rho(J, T)$ is the triplet density, i.e., the probability for a given dimer to be in triplet state.[23] The triplet density, disregarding Zeeman and ZFS energies, is $\rho = [1 + (\exp(-J/kT))/3]^{-1}$, which for a singlet−triplet splitting $J = +3.2$ cm^{-1} at room temperature has a value $\rho \approx 0.75$. With this in consideration, we calculated $J' = (0.0070 \pm 0.0003)$ cm^{-1} for the interdimeric exchange constant mediated by the hydrophobic interaction between two neighboring phen molecules, using the ω_{ex} obtained from the data in the *ca** plane.

EPR Spectra in the $g_\perp$ Region. In the absence of interdimeric exchange, the EPR line width in Cu(tda)(phen) is determined by the square root of the sum of the second moment of the dipolar and hyperfine interactions. The second moment of the hyperfine interaction is proportional to the $\mathbf{A}^2$-tensor with **A**- and **g**-tensors being roughly coincident in copper compounds. The angular variation of M_2^{dip} is shown in Figure S3.[42,43] For Cu(tda)phen, the contribution of both interactions to the EPR line width in the $g_\perp$ region is minimal and of the order of ∼45 G, which allows a better evaluation of the interdimeric exchange interaction effects on the resonance lines in this region.

In the $g_\perp$ region of the *ca** plane, a single Lorentzian line would be expected as the maximal separation between the triplet resonance lines predicted by eq 2 is approximately similar to that of $\theta = 5°$ and $\theta = 75°$ (Figure 5a), angles at which a single line is observed ($\delta/\omega_{ex} \sim 1$). However, the spectra in the $g_\perp$ region do show a single resonance line at the center of the spectra, as expected for situations with $\delta/\omega_{ex} \sim 1$, but present in addition two symmetrical shoulders at both sides of the central line (see Figure 4, spectrum c), suggesting spectra associated with dimers in weak exchange regime ($\delta/\omega_{ex} > 1$). This particular situation was rationalized using a more general approach considering the different contributions to the spectra of dimers in different conditions. The exact probability P_n for each dimer of being surrounded by *n* dimers in triplet state is given by the binomial distribution

$$P_n = \frac{4!}{(4-n)!n!}\rho^n(1-\rho)^{4-n} \qquad (7)$$

According to eq 7 and considering $\rho = 0.75$, 31.6% of the dimers are surrounded by four triplets ($n = 4$), 42.2% by three triplets ($n = 3$), 21% by two triplets ($n = 2$), and 5% by one triplet ($n = 1$), and a negligible percentage is not surrounded

by any triplet. These dimer populations experience different interdimeric exchange interactions given by $\omega_{ex,n} = nJ'$, and hence $I(\omega)$ can be obtained through the weighted sum of the contributions of each dimer population

$$I(\omega) = \sum_n P_n I(\omega, \omega_{ex,n}) \quad (8)$$

where $I(\omega, \omega_{ex,n})$ is the same as in eq 5 but evaluated for each $\omega_{ex,n}$.

Spectral simulation with eq 8 using $J' = 0.0070$ cm^{-1} for the selected spectra in the *ca** plane is shown in Figure 4. Note that although the number of parameters involved in eq 8 is high and some parameters (line widths) are difficult to evaluate for each n, simulation can reproduce reasonably well the experimental spectra. Particularly, simulation of spectrum c shows that the central single resonance line is determined principally by dimers in the strong exchange situation ($\delta/\omega_{ex} = \delta/4J' < 1$), while the shoulders originate from the contribution of dimers in weak exchange situation ($\delta/nJ' > 1$, where $n = 1$, 2, and 3). Except for the central line, the simulated positions and widths of the satellite lines show some discrepancy with the experimental ones, probably originating from the use of the point dipole approximation that disregards covalency effects of the ligands and the assumption of a unique interdimeric exchange constant J'. In any case, the good agreement obtained between experiment and simulation using eq 8 in the 15°−60° range in the *ca** plane (see, e.g., Figure 4, spectrum a) confirms that the simpler method based on eq 5 can satisfactorily be used to obtain the interdimeric exchange constant in those situations where the satellite features of dimer spectra are either folded into the EPR line width or negligible because of the higher intensity of the central line.

Conclusions

EPR measurements on powdered and on oriented single crystal samples of the compound Cu(tda)(phen) show how the EPR triplet transitions of a dimeric system are modulated by weak interdimeric exchange interactions. From the angular variation of the interdimeric exchange collapsed spectra, we determined the molecular **g**-tensor of the copper ions and showed that the fine structure of the dimer originates mainly from the intradimeric dipolar interaction. The single crystal EPR spectra were interpreted using Anderson's model of exchange narrowing, which allowed us, together with statistical arguments, to demonstrate that the interdimer exchange interaction experienced by each molecular unit depends on the number of neighboring dimers in triplet states. We evaluated an interdimeric exchange constant $J' = 0.0070$ cm^{-1} associated with the hydrophobic interaction between two 1,10-phenanthroline molecules. The triplet EPR spectra corresponding to the isolated dimer are significantly modified by this interaction, indicating that this chemical path can transmit weak magnetic interactions between copper(II) centers at relatively long distances of the order of ~10 Å. Since similar distances between metal centers connected by chemical paths involving hydrophobic interactions can be found in several redox metalloproteins, these results may also be useful to understand and elucidate the most efficient electron transfer pathways in such biological systems.

Acknowledgment. We thank FONCyT, CONICET, and CAI+D-UNL for financial support. We thank the Spanish Research Council (CSIC) for providing a free of charge license to the Cambridge Structural Database.[44] N.I.N. thanks CONICET for a fellowship grant. M.P. and C.D.B. are members of CONICET-Argentina.

Supporting Information Available: Figures containing EPR spectra obtained in the *ca** and *cb* crystal planes, spectral simulations in the range 15−60° of the *ca** plane using the derivative of eq 5, angular variation of the square root of the dipolar second moment in three crystal planes, and a table with the eigenvalues and eigenvectors of the **D**-tensors. This material is available free of charge via the Internet at http://pubs.acs.org.

References and Notes

(1) Kim, E.; Chufan, E. E.; Kamaraj, K.; Karlin, K. D. *Chem. Rev.* **2004**, *104*, 1077–1134.
(2) Mrozinski, J. *Coord. Chem. Rev.* **2005**, *249*, 2534–2548.
(3) Chen, P.; Solomon, E. I. *Proc. Natl. Acad. Sci. U.S.A.* **2004**, *101*, 13105–13110.
(4) Verdaguer, M. *Polyhedron* **2001**, *20*, 1115–1128.
(5) Abragam, A.; Bleaney, B. *Electron Paramagnetic Resonance of Transition Ions*; Oxford University Press: Oxford, England, 1970.
(6) Bencini, A., Gatteschi, D. *Electron Paramagnetic Resonance of Exchange Coupled Systems*; Springer-Verlag: Berlin, Germany, 1990.
(7) Kahn, O. *Molecular Magnetism*; VCH Publishers: New York, 1993.
(8) Ceulemans, A.; Chibotaru, L. F.; Heylen, G. A.; Pierloot, K.; Vanquickenborne, L. G. *Chem. Rev.* **2000**, *100*, 787–806.
(9) Wichmann, O.; Sopo, H.; Colacio, E.; Mota, A. J.; Sillanpää, R. *Eur. J. Inorg. Chem.* **2009**, *2009*, 4877–4886.
(10) Perec, M.; Baggio, R.; Sartoris, R. P.; Santana, R. C.; Peña, O.; Calvo, R. *Inorg. Chem.* **2010**, *49*, 695–703.
(11) Koval, I. A.; van der Schilden, K.; Schuitema, A. M.; Gamez, P.; Belle, C.; Pierre, J.-L.; Luken, M.; Krebs, B.; Roubeau, O.; Reedijk, J. *Inorg. Chem.* **2005**, *44*, 4372–4382.
(12) Schlam, R. F.; Perec, M.; Calvo, R.; Lezama, L.; Insausti, M.; Rojo, T.; Foxman, B. M. *Inorg. Chim. Acta* **2000**, *310*, 81–88.
(13) Owen, J., Harris, E. A. Pair Spectra and Exchange Interaction. In *Electron Paramagnetic Resonance*; Geschwind, S., Ed.; Plenum Press: New York, 1972.
(14) Napolitano, L. M. B.; Nascimento, O. R.; Cabaleiro, S.; Castro, J.; Calvo, R. *Phys. Rev. B: Condens. Matter Mater. Phys.* **2008**, *77*, 214423–214413.
(15) Boillot, M. L.; Journaux, Y.; Bencini, A.; Gatteschi, D.; Kahn, O. *Inorg. Chem.* **1985**, *24*, 263–267.
(16) Hilczer, W.; Goslar, J.; Tritt-Goc, J.; Hoffmann, S. K. *Inorg. Chem.* **1995**, *34*, 1852–1858.
(17) Valentine, J. S.; Silverstein, A. J.; Soos, Z. G. *J. Am. Chem. Soc.* **1974**, *96*, 97–103.
(18) Calvo, R. *Appl. Magn. Reson.* **2007**, *31*, 271–299.
(19) Hoffmann, S.; Hilczer, W.; Goslar, J. *Appl. Magn. Reson.* **1994**, *7*, 289–321.
(20) McInnes, E. J. L.; Mabbs, F. E.; Grant, C. M.; Milne, P. E. Y.; Winpenny, R. E. P. *J. Chem. Soc., Faraday Trans.* **1996**, *92*, 4251–4256.
(21) Hoffmann, S. K.; Hodgson, D. J.; Hatfield, W. E. *Inorg. Chem.* **1985**, *24*, 1194–1201.
(22) Lynden-Bell, R. M.; McConnell, H. M. *J. Chem. Phys.* **1962**, *37*, 794–798.
(23) McConnell, H. M.; Lynden-Bell, R. *J. Chem. Phys.* **1962**, *36*, 2393–2397.
(24) Baggio, R.; Garland, M. T.; Manzur, J.; Peña, O.; Perec, M.; Spodine, E.; Vega, A. *Inorg. Chim. Acta* **1999**, *286*, 74–79.
(25) Stoll, S.; Schweiger, A. *J. Magn. Reson.* **2006**, *178*, 42–55.
(26) Macrae, C. F.; Bruno, I. J.; Chisholm, J. A.; Edgington, P. R.; McCabe, P.; Pidcock, E.; Rodriguez-Monge, L.; Taylor, R.; van de Streek, J.; Wood, P. A. *J. Appl. Crystallogr.* **2008**, *41*, 466–470.
(27) Weil, J. A., Bolton, J. R. *Electron Paramagnetic Resonance*, 2nd ed.; John Wiley & Sons: Hoboken, NJ, 2007.
(28) Vicente, M.; Bastida, R.; Macías, A.; Valencia, L.; Geraldes, C. F. G. C.; Brondino, C. D. *Inorg. Chim. Acta* **2005**, *358*, 1141–1150.
(29) Tamayo, A.; Casabó, J.; Escriche, L.; González, P.; Lodeiro, C.; Rizzi, A. C.; Brondino, C. D.; Passeggi, M. C. G.; Kivekäs, R.; Sillanpää, R. *Inorg. Chem.* **2007**, *46*, 5665–5672.
(30) Carrington, A.; McLachlan, A. D. *Introduction to Magnetic Resonance*, 1st ed.; Harper & Row: New York, 1967.
(31) Folgado, J. V.; Ibanez, R.; Coronado, E.; Beltran, D.; Savariault, J. M.; Galy, J. *Inorg. Chem.* **1988**, *27*, 19–26.
(32) Brondino, C. D.; Calvo, R.; Atria, A. M.; Spodine, E.; Peña, O. *Inorg. Chim. Acta* **1995**, *228*, 261–266.

(33) Brondino, C. D.; Calvo, R.; Atria, A. M.; Spodine, E.; Nascimento, O. R.; Peña, O. *Inorg. Chem.* **1997**, *36*, 3183–3189.
(34) Anderson, P. W.; Weiss, P. R. *Rev. Mod. Phys.* **1953**, *25*, 269.
(35) Anderson, P. W. *J. Phys. Soc. Jpn.* **1954**, *9*, 23.
(36) Abragam, A. *The Principles of Nuclear Magnetism*; Oxford University Press: London, 1961.
(37) Sack, R. A. *Mol. Phys.* **1958**, *1*, 163–167.
(38) Hoffmann, S. K.; Waskowska, A.; Hilczer, W. *Solid State Commun.* **1990**, *74*, 1359–1361.
(39) Calvo, R.; Mesa, M. A. *Phys. Rev. B* **1983**, *28*, 1244.
(40) Bonomo, R. P.; Rizzarelli, E.; Bresciani-Pahor, N.; Nardin, G. *J. Chem. Soc., Dalton Trans.* **1982**, 681–685.
(41) Baggio, R.; Calvo, R.; Garland, M. T.; Peña, O.; Perec, M.; Slep, L. D. *Inorg. Chem. Commun.* **2007**, *10*, 1249–1252.
(42) Gennaro, A. M.; Calvo, R. *J. Phys.: Condens. Matter* **1989**, *1*, 7061–7068.
(43) Gennaro, A. M.; Calvo, R. *J. Phys.: Condens. Matter* **1990**, 2873.
(44) Allen, F. *Acta Crystallogr., Sect. B* **2002**, *58*, 380–388.

JP108736P